

Cite this: *Dalton Trans.*, 2022, **51**, 14182Received 1st August 2022,  
Accepted 29th August 2022

DOI: 10.1039/d2dt02501a

rsc.li/dalton

# On the non-existence of a square-planar pentaiodide coordination complex $I(I)_4^-$ †

Lars Kloo 

The properties of two conformers of the pentaiodide ion, a V-shaped and regularly observed  $I_5^-$  ion, and a so far undetected square-planar coordination complex of  $II_4^-$  composition, have been investigated by computational methods. The latter compound is indicated by the analogy to the coordination chemistry of gold with halide ligands, as well as isoelectronic main-group compounds. Static and dynamic simulations at density-functional and semi-empirical level including effects of solvent and counter ions indicate that the square-planar  $II_4^-$  indeed represents a well-defined local minimum on the pentaiodide potential energy surface, albeit less stable than the typically observed V-shaped  $I_5^-$ . No simple pathway of transformation between the two forms of the pentaiodide ion can be identified. Molecular dynamics simulations indicate that the presence of cations, unavoidable during the synthesis of polyiodide compounds, may trigger decomposition of the  $II_4^-$  coordination complex into smaller polyiodide building blocks and thus constitute the main reason why this conformer so far has not been identified in solid polyiodide compounds. However, its intrinsic stability indicates that the square-planar form should be possible to isolate in solid compounds given the right conditions of synthesis.

## Introduction

Polyhalide compounds in general and polyiodides in particular offer a rich structural chemistry of catenated, low-dimensional compounds.<sup>1,2</sup> The vast majority of polyiodide compounds can be visualized in terms of simple coordination chemistry, in which the ionic building blocks of  $I^-$  and  $I_3^-$  can be regarded as solvated by the neutral solvent molecules  $I_2$ . The sticky bonding properties of the relatively small and few building blocks generate chain-like structures, which can be attributed to topological electron densities of the building blocks ( $\sigma$ -holes).<sup>2,3</sup> The predominant bonding contributions have been assigned to secondary interactions, such as dispersion and induction, complemented by weak covalency mediated by overlap of the large valence orbitals of iodine.<sup>4</sup> However, this scheme has recently been challenged and the bonding been solely attributed to non-covalent interactions.<sup>5</sup>

More specifically, a large number of compounds named as pentaiodides can be found in a search of the Cambridge Structural Database (CSD).<sup>6</sup> The denotation pentaiodide refers primarily to the stoichiometry with respect to a suitable monocation, often a small organic cation. However, even such a simple stoichiometry offers a large diversity in terms of geo-

metric structure. The stoichiometric pentaiodides can be found as isolated ions or as the repeating unit in typically chain-like structures, and they can be described as either of V-shape  $[(I^-) \cdot 2I_2]$  or of L-shape  $[(I_3^-) \cdot I_2]$ , see Fig. 1.<sup>1</sup>

Alongside the catenated chemistry of polyiodides, there is an interesting analogy between the coordination chemistry of interhalogen compounds and gold-halide complexes. For instance, the well-known, linear gold(i) complexes  $AuCl_2^-$  and  $AuI_2^-$  can be compared to the interhalogen ions (complexes)  $ICl_2^-$  and  $II_2^-$  (*i.e.* the triiodide ion  $I_3^-$ ) in the sense that they are structurally highly similar and the coordination centre can be regarded to be in a +I oxidation state. The view of iodine in a formal positive oxidation state as a coordination centre has recently been highlighted in comparison to that of silver(i), as well as to gold(i and iii).<sup>7,8</sup> In fact, the mixed anion, or as it might better be described as the iodide-bridged, gold(i)-iodide species  $Au_2I_3^-$  is structurally analogous to the V-shaped pentaiodide ion.<sup>9</sup> I analogy, the square-planar gold(iii) complexes  $AuCl_4^-$  and  $AuI_4^-$  can be compared to  $ICl_4^-$  and  $II_4^-$  (*i.e.* another structural form of the pentaiodide ion  $I_5^-$ ), see Fig. 2. However, here there is one clear discrepancy, the pentaiodide ion has to our knowledge so far not been found as a square-planar coordination complex, but rather in the forms shown in Fig. 1. Why not?

In this context, it is relevant to mention some analogies to similar and isoelectronic main-group compounds. Regarding valence electron numbers, a square-planar  $II_4^-$  can be thought of as a congener to the well-known, square-planar molecules  $SF_4^{2-}$  and  $XeF_4$ ; compounds that essentially every undergradu-

Applied Physical Chemistry, Department of Chemistry, KTH Royal Institute of Technology, SE-100 44 Stockholm, Sweden. E-mail: Lakloo@kth.se

† Electronic supplementary information (ESI) available. See DOI: <https://doi.org/10.1039/d2dt02501a>



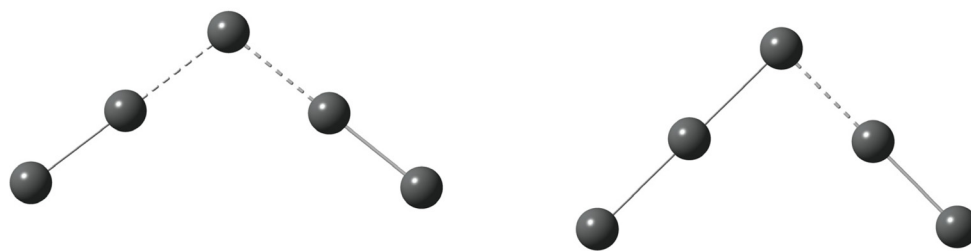


Fig. 1 Penta-iodide ions in V-shaped (left) or L-shaped (right) forms; isolated or as part of an extended, chain-like structure; iodine atoms (grey).

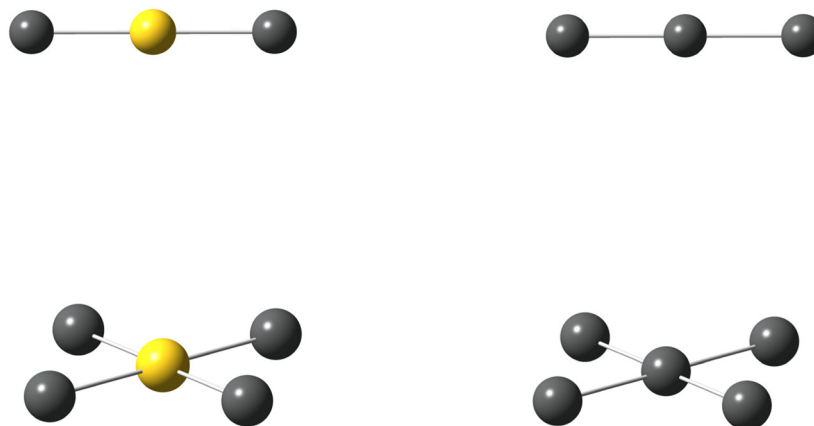


Fig. 2 The well-known, linear  $\text{AuI}_2^-$  (top left), square-planar  $\text{AuI}_4^-$  complex (bottom left) and triiodide ion  $\text{I}_3^-$  (top right), as well as a hypothetical analogous  $\text{I}_4^-$  ion (bottom right); gold atoms (yellow), iodine atoms (grey).

ate student in introductory chemistry has been exposed to when introduced to chemical bonding and Lewis electron structures. Among interhalogen compounds, the square-planar configuration is observed for a series of  $\text{XF}_4^-$  compounds ( $\text{X} = \text{Cl}, \text{Br}$  or  $\text{I}$ ) and the above noted  $\text{ICl}_4^-$  ion; where a characteristic property is that the most electronegative element is found in the terminal positions; all akin to the  $\text{I}_4^-$  form of the penta-iodide ion. The analogies to the halides of the chalcogenides also include the closely related, square-planar halide complexes of tellurium, *viz.*  $\text{TeI}_4^{2-}$ , that were synthesized and structurally characterized by Krebs and co-workers.<sup>10</sup> In this context, also the unique and to this work relevant gold coordination compound with noble-gas ligands,  $\text{AuXe}_4^{2+}$  isolated by Seppelt and Seidel, should be mentioned.<sup>11</sup>

A search of the CSD for square-planar  $\text{I}_5$  structural fragments offers no relevant hits. A handful of structures can be described in terms of catenated penta-iodide fragments with a coordination resembling that of a distorted tetrahedron, but none can be regarded as an isolated square-planar  $\text{I}_4^-$  complex. As will be shown below, such a penta-iodide coordination complex resides in a well-defined minimum on the penta-iodide potential energy surface (PES), albeit energetically less stable than the V-shaped form shown in Fig. 1. This work will attempt to answer the question why such a coordination species has not been found among the many penta-iodide structures known; at least not yet.

## Computational

Most quantum chemical computations of static models were performed using Gaussian 16 (Rev. B.01 and C.01).<sup>12</sup> ECP-based basis sets were used for I and Au employing the Stuttgart–Dresden–Cologne group, relativistic, effective-core potentials (ECPs; MDF60 for Au and MDF28 for I) and valence spaces of (14s11p10d3f2g1h)/[6s6p5d3f2g1h] quality for Au,<sup>13,14</sup> and (14s11p12d2f1g)[6s6p4d2f1g] for I.<sup>15</sup> Calculations were performed at density-functional theory (DFT) level using the hybrid functional cam-B3LYP.<sup>16</sup> 2nd order relativistic effects including spin-orbit coupling were considered using and the def2-QZVP/def2-QZVP-2c basis sets and associated ECPs for iodine including spin-orbit coupling coefficients and based on the Gaussian formulation of the hybrid functional B3LYP as implemented in Turbomole 7.2.<sup>17–20</sup> Molecular dynamics simulations were performed at DFT level using TeraChem v1.9-2021.05 employing the hybrid functional B3LYP and ECP-based basis sets of single-valence quality.<sup>21,22</sup> A Langevin thermostat was employed at a fixed nominal temperature and a time step of 1 fs extending to in total 100 ps of simulation starting with an optimized structure of the system under study. Semi-empirical molecular dynamics simulations were performed using the xTB v.6.4.0 at GFN2 level in an NVT ensemble and a Berendsen thermostat.<sup>23,24</sup> The acetone droplets consisting of 100 acetone molecules with the density of



pure acetone were constructed using Packmol, and the solutes were confined to the droplet centre in the xTB simulations.<sup>25</sup> Also the semi-empirical simulations were extended to 100 ps with 1 fs time steps, and data were collected at every 50 fs. Both TeraChem and xTB were operated on graphical processor units.

Analyses of the computed molecular orbitals were made using the Natural Bond Order (NBO) and Natural Energy Decomposition Analysis (NEDA) functionalities in NBO 7.0 as interfaced with Gaussian 16.<sup>26</sup> Results from the simulations were visualized using VMD 1.9 and GaussView 6.<sup>27,28</sup> Details on the evolution of atom-atom distances with simulation time in the different systems studied are provided in the ESI.†

## Results and discussion

### Energies of the conformers

The initial investigation was performed to identify if a potential, square-planar  $\text{II}_4^-$  complex at all is energetically feasible with respect to both the most stable conformer, the V-shaped  $\text{I}_5^-$  ion, as well as with respect to the fragments  $\text{I}_3^-$  and  $\text{I}_2$  and the fundamental fragments consisting of one  $\text{I}^-$  ion and two  $\text{I}_2$  molecules. The relative total energies compared to the V-shaped  $\text{I}_5^-$  ion are collected in Table 1.

We can extract two pieces of qualitative information from the results in Table 1; first, both molecular ions are stable relative the components of an iodide ion and two iodine molecules, albeit the square-planar  $\text{II}_4^-$  is slightly less stable than the combination of a triiodide ion and an iodine molecule; second, the square-planar  $\text{II}_4^-$  complex is energetically stable, though less so than the commonly found V-shaped structure and should therefore be regarded as a meta-stable form of the penta iodide ion. Although inclusion of spin-orbit coupling significantly shifts the total energies of the systems, the relative energies remain essentially unchanged and therefore do not alter these conclusions. In this context, it can be noted that the square-planar  $\text{II}_4^-$  complex displays no negative eigenvalues in the Hessian upon a vibrational spectroscopic analysis, and the totally symmetric vibration mode can be found at  $118\text{ cm}^{-1}$ , which because of significant overlap with typical polyiodide Raman bands would be difficult to single out in a normal Raman spectrum of a polyiodide system. Nevertheless,  $\text{II}_4^-$  represents a true (local) minimum on the PES of the penta iodide ion system.

Bonding analyses of the V-shaped and square-planar penta iodide forms using NBO7 and NEDA show a significant degree of covalency in both ions with Wiberg bond indices of 0.33 and 0.45, between the top/central iodine atom and the closest neighbours, respectively, and a corresponding NLMO bond order of 0.20 and 0.34. As a reference, from electron counts based on simple molecular-orbital diagrams one would expect the corresponding I-I bond order in  $\text{I}_2$  to be 1 and in a centrosymmetric and linear  $\text{I}_3^-$  to be 1/2. The Wiberg and NLMO bond indices, as anticipated, emerge as 1.03/1.01 and 0.53/0.52, respectively, for the two molecular systems. NEDA analyses of the energy contributions to the interaction energy for the V-shaped  $\text{I}_5^-$  ion and  $\text{I}_3^-$  (the latter, although centrosymmetric, treated as an  $\text{I}^-$ - $\text{I}_2$  unit) show that the charge-transfer contributions to the overall bonding energy are quite similar in the two systems, indicating that covalent interaction contributes significantly to the interaction between the  $\text{I}^-$  ion and the two iodine molecules in the V-shaped  $\text{I}_5^-$  polyiodide ion. In the square-planar conformer, the charge-transfer contribution is significantly higher and dominates completely with a factor of about 8 with respect to polarization contributions.

It can be noted that although different types of frontier orbitals will be predominant bonding orbitals in the two analogous, square-planar  $\text{AuI}_4^-$  and  $\text{II}_4^-$  complexes, from a qualitative point of view the bonding scheme will be similar. Bonding in polyhalides is typically dominated by the halogen p-orbitals, as shown by Pimentel, Rundle and others.<sup>29,30</sup> Thus, visualizing the ligand iodine atoms as iodide ions, they will predominantly dominate electron density from their filled p-orbitals into available empty orbitals on the central atom, *viz.*  $\text{Au}(+3)$  or  $\text{I}(+3)$ . The available orbitals on gold(III) will be d-orbitals (*i.e.* the  $d(x^2-y^2)$ -orbital) and on iodine(III) p-orbitals (*i.e.* the p(x)- and p(y)-orbitals), if assigning bonding to the (x, y)-plane. In terms of electron density, the resulting systems will be highly similar, although symmetry will of course differ considering that d-orbitals are centrosymmetric and p-orbitals are not, as highlighted in Fig. 3.

### Transitions

Having established that the square-planar conformer of the penta iodide ion is energetically feasible representing a local energy minimum on the penta iodide PES, a logical next step will be to investigate if there is a straightforward route of transition between the square-planar and the commonly observed V-shaped conformers. Two different approaches were utilized.

The first approach described in this section involved the extraction or addition of  $\text{I}_2$  units to an  $\text{I}_3^-$  core placing the iodine molecule either with all atoms in the same plane or the  $\text{I}_2$  unit perpendicularly to the triiodide ion. As is obvious from Fig. 4, in none of the investigated systems a straightforward pathway from or to the square-planar  $\text{II}_4^-$  by addition of or extraction of a neutral  $\text{I}_2$  molecule can be identified. In addition, none of the nine normal vibrational modes of the square-planar  $\text{II}_4^-$  ion offer any insights as for potential routes of transformation into a more commonly encountered form of the penta iodide ion.

**Table 1** Relative total energies of the different forms of a penta iodide system, also including the effects of relativistic spin-orbit coupling

$\text{I}_5^-$ system	No spin-orbit coupling		Spin-orbit coupling $\Delta E/\text{eV}$
	I-I distance/Å	$\Delta E/\text{eV}$	
$(\text{I}^-)\cdot 2\text{I}_2$ , V-shaped	2.815, 3.093	0	0
$\text{II}_4^-$ , square-planar	2.923	+0.94	+0.91
$\text{I}^-$ & two $\text{I}_2$	2.663	+2.09	+2.08
$\text{I}_3^-$ & $\text{I}_2$	2.663, 2.952	+0.67	+0.67



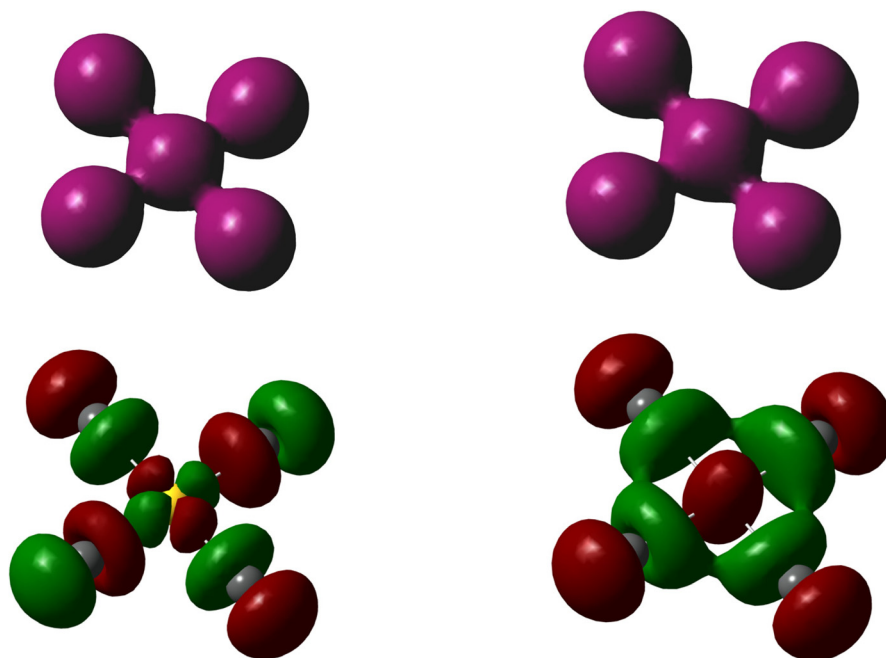


**Fig. 3** The total electron density surfaces of AuI<sub>4</sub><sup>-</sup> (top left) and II<sub>4</sub><sup>-</sup> (top right), and the corresponding surfaces of the highest occupied molecular orbitals (HOMOs, bottom); iso-surface values used are 0.04 e/(au)<sup>3</sup> for the total electron density and 0.025 [e/(au)<sup>3</sup>]<sup>1/2</sup> for the molecular orbitals.

The second type of analysis described in the subsequent section will involve molecular dynamics at *ab initio* and semi-empirical level in order to allow the investigation of the effects of dynamics, as well as potentially allow the identification of reaction routes of inter-conversion not formulated *a priori*.

### Dynamics

In the above analysis, the isolated polyiodide fragments were investigated. However, in real-life syntheses both solvent and counter ions are involved, and in this section such effects will be taken into account.

The first molecular dynamics simulations at *ab initio* level focussed on the isolated V-shaped and square-planar penta-iodide units extending to 100 ps. A primitive methodology to provoke reactive events is to increase the nominal simulation temperature in order to increase the probability of reaction events to take place. Therefore, the simulations at ambient temperature were complemented by further ones at 300 and 600 °C. The square-planar II<sub>4</sub><sup>-</sup> ion remained intact during all simulations emphasizing that it should be regarded as a locally highly stable entity. However, upon increasing the simulation temperature for the V-shaped and commonly encountered I<sub>5</sub><sup>-</sup> ion, that ion showed an increasing tendency to split into its expected and smaller building blocks, I<sub>3</sub><sup>-</sup> and I<sub>2</sub>; at 600 °C, that separation was observed (towards the end of the simulation time) and persisted throughout the simulation time (see Fig. S1† for more details). This may reflect that the square-planar II<sub>4</sub><sup>-</sup> ion does not have well-defined reaction pathways with relatively low reaction barriers to smaller fragments, whereas the V-shaped I<sub>5</sub><sup>-</sup> does.

When synthesizing polyiodides, useful solvents are polar organic molecular systems, such as ethanol or acetone. It is therefore a natural first extension of the study to involve a solvent in the molecular dynamics studies. Acetone was selected as a suitable system, since it is commonly employed in polyiodide synthesis and will not complicate the polyiodide system by strong hydrogen bonding (known to have effects on the speciation and the structure of polyiodide compounds synthesized). A droplet consisting of 100 acetone molecules at a typical density for the solvent was constructed and the two conformers of the penta-iodide ion were placed in the system centres. The systems are quite big, and therefore semi-empirical simulations were employed. The simulations were extended to 100 ps at ambient temperature, see Fig. 5 and Fig. S2.† Again, the square-planar II<sub>4</sub><sup>-</sup> complex remained intact over the entire time of simulation, whereas the V-shaped I<sub>5</sub><sup>-</sup> almost immediately split into the expected I<sub>3</sub><sup>-</sup> and I<sub>2</sub> fragments with I<sub>2</sub> diffusing to the outer rim of the acetone droplet.

As a side-comment, the diffusion of hydrophobic entities to the droplet rim during simulations in polar solvent models is a quite common phenomenon, in particular when studying biomolecules in water. Sometimes this is referred to as vacuum being hydrophobic. However, that is not a fully accurate description of the driving forces for the observed effect, since it is essentially the molecule-molecule interactions between the polar solvent components that are disturbed or reduced, and as a consequence the less polar solutes are pushed to the position where they interfere with the intrinsic solvent interactions the least, *i.e.* to the outskirts of the droplet. This is also the phenomenon that we observe for the I<sub>2</sub> unit split off from the V-shaped I<sub>5</sub><sup>-</sup> ion. In



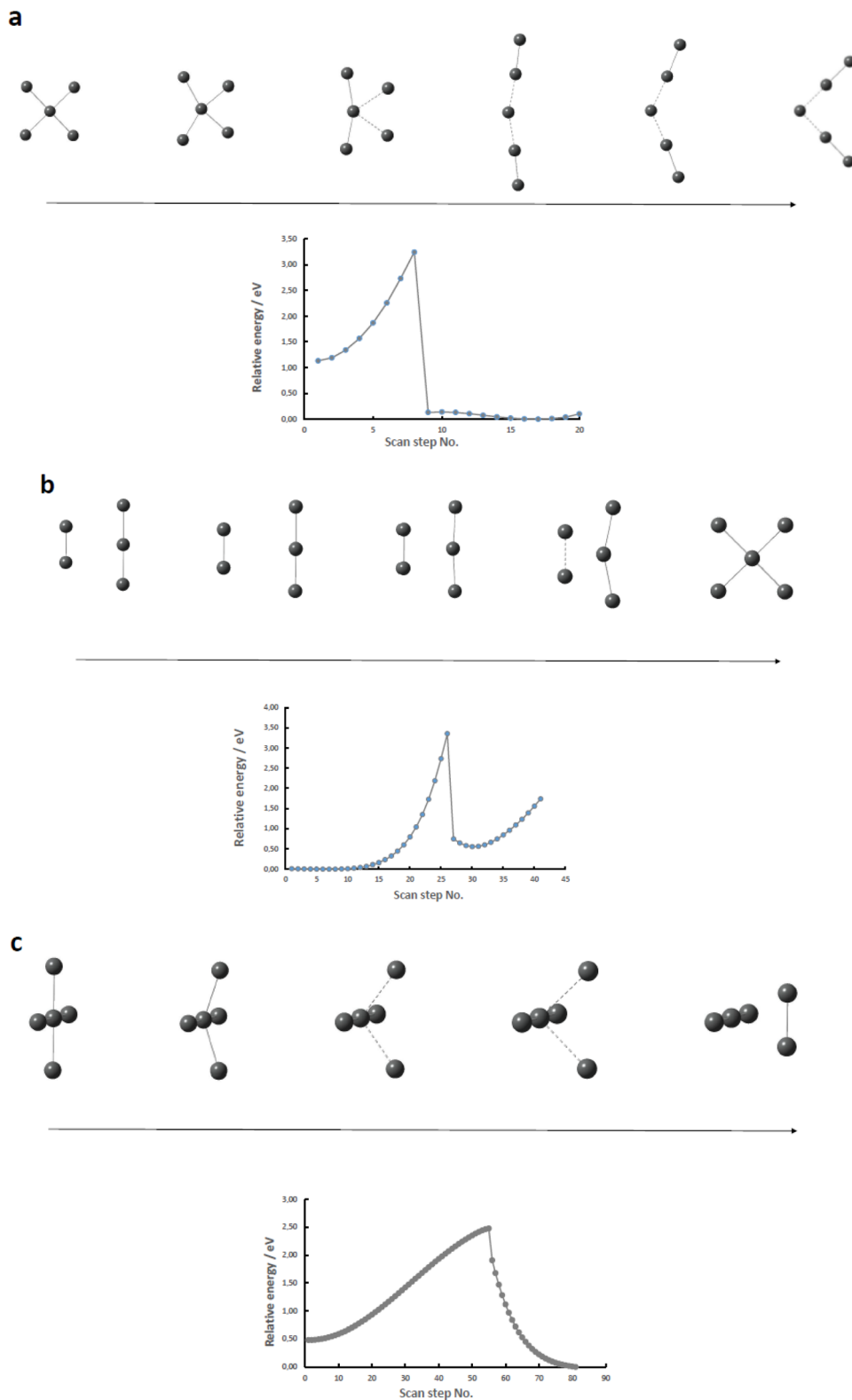


**Fig. 4** Relative energy scans of (a) in-plane  $I_2$  extraction from  $I_4^-$ ; (b) in-plane  $I_2$  addition to  $I_3^-$ ; (c) perpendicular extraction of  $I_2$  from  $I_4^-$  (with a linearly restricted  $I_3^-$  unit); iodine atoms (grey).



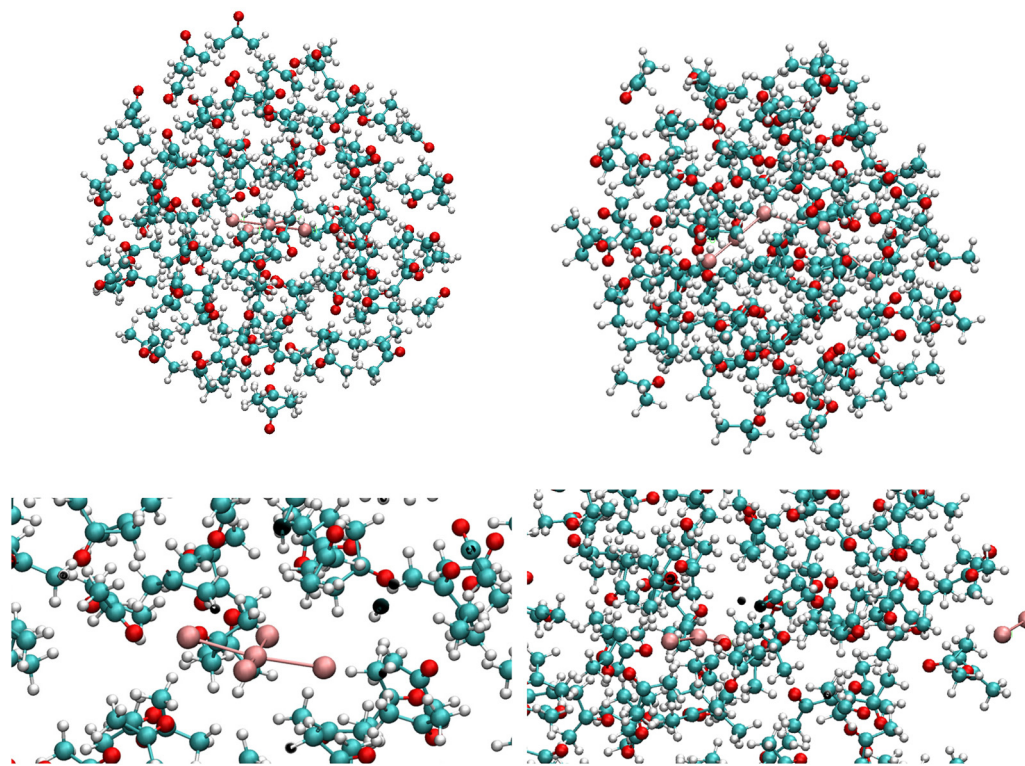


**Fig. 5** The two initial models of square-planar  $I_4^-$  (top left) and V-shaped  $I_5^-$  (top right), and the end results after 100 ps simulation under ambient conditions (bottom left and right, respectively); iodine atoms (bronze; different atom colour from the other figures for sake of clarity).

summary, we observe the same trends as noted for the non-solvated pentaiodide ions, although the polar solvent accentuates the tendency of the V-shaped  $I_5^-$  ion to decompose into  $I_3^-$  and  $I_2$  also at low simulation temperatures.

In polyiodide synthesis of course electroneutrality must be fulfilled, and thus the anionic reactants are by necessity accompanied by cationic counter ions. It is also in this aspect that the use of polar organic solvents makes sense, since they are good solvents for both the iodide salts and for the more non-polar iodine molecules. Depending on what type, structure and size of polyiodide is your target product, different cations and solvents can be selected. In the subsequent study, two quite different types of simple cations have been selected for aiMD simulations,  $Li^+$  and  $Au^+$ . The lithium cation was selected because it is small and polarizing, and therefore will enhance any disrupting effects of a cation on the pentaiodide structures. It is well known from literature that cations of this type interact strongly with the polyiodide fragments and often in a bridging position between the ionic and neutral building blocks (like between the  $I^-$  and  $I_2$  fragments). In this section, only the square-planar pentaiodide system was studied, since the interactions of the V-shaped pentaiodide with cations is well investigated and described in the literature. Thus, the main target is to provoke any type of reaction of the square-planar  $I_4^-$  complex in the presence of cations in order to extract insights into the reasons why such a species has not

been observed albeit that it obviously, if formed, should be considerably stable.

The aiMD simulations for the anionic  $I_4^-$  system was repeated at ambient temperature and at 300 °C, but no reactions could be observed. However, at 600 °C, the square-planar  $I_4^-$  eventually split into the notorious building blocks  $I_3^-$  and  $I_2$ , where the  $I_3^-$  ion is coordinated by the  $Li^+$  ion in the expected asymmetric coordinating position found in most solid polyiodide structures, see Fig. 6 and Fig. S3.† The dynamics of decomposition is not straightforward; after approximately 40 ps of simulation  $LiI$  splits off from the system leaving the remaining four iodine atoms in a less ordered heap, whereafter  $LiI$  again approaches the iodine heap to extract away an  $I_2$  entity and as a result the  $Li-I_3$  and  $I_2$  units diffuse away from each other. Further details are given in Fig. S3 in the ESI.† The main conclusion is that cation interaction very well may disfavour the formation of the square-planar  $I_4^-$  complex to the benefit of the regularly known, chain-like polyiodide building blocks.

The  $Au^+$  ion was included mainly for two reasons; first, it represents a completely different type of cation than  $Li^+$ ; 2, the resemblance of the gold and iodine coordination chemistry may provide some new insights into the interaction between gold and iodine in the combined systems. Indeed, already at ambient conditions complex reactions can be observed; not always with easily interpreted results in terms of expected coordination compounds, though. At 25 °C,  $Au^+$  almost



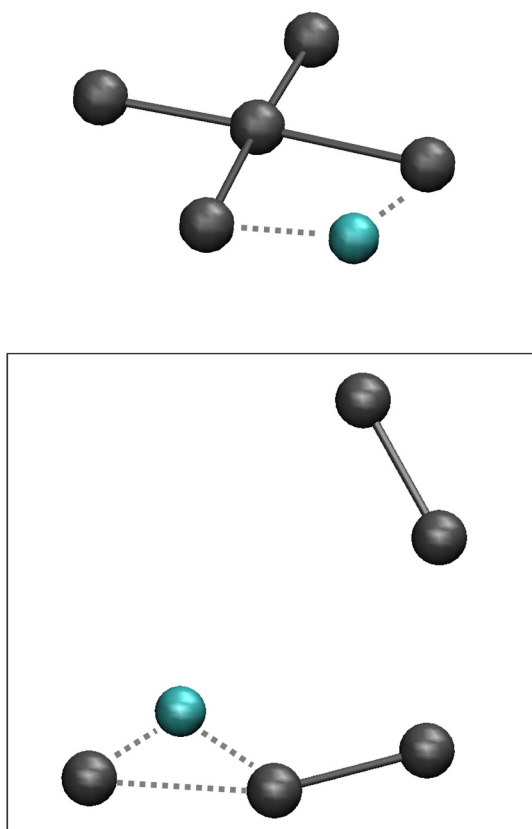


**Fig. 6** The initial  $\text{Li}^+\text{-I}_4^-$  model as obtained from static geometry optimization (top), and a snapshot of the end products after approximately 60 ps simulation; iodine atoms (grey), lithium atoms (cyan).

immediately becomes integrated into the  $\text{I}_4^-$  structure forming a linear  $\text{AuI}_2^-$  type of entity at the edge, but with unclear interaction with the remaining three iodine atoms.

After about 50 ps of simulation  $\text{I}_2$  is separated from the other atoms leaving behind, from a coordination chemistry point of view, a rather obscure entity; an odd-looking  $\text{AuI}_3^-$ , see Fig. 7. Comparisons to regular  $\text{AuI}_2^-$  and  $\text{AuI}_4^-$  complexes, as well as to a more non-intuitive  $\text{AuI}(\text{I}_2)$  unit consisting of  $\text{Au}^+$  coordinated by an iodide ion on the one side and an iodine molecule on the other, the latter constellation comes out as the most likely end product in the aiMD simulation. A separately constructed and geometrically optimized  $\text{AuI}(\text{I}_2)$  complex at DFT level offers highly analogous results. Both NBO charges and atom-atom distances match the end product of the MD simulation quite well (Au, I and  $\text{I}_2$ : +0.29, -0.44, and close to zero in the simulation, +0.34, -0.40 and close to zero in the optimized structure; Au-I, Au- $\text{I}_2$  and I-I: 2.589, 2.615 and 2.897 Å in the simulation, 2.537, 2.623 and 2.712 Å in the optimized structure). The simulations at higher temperatures display the same outcome, although arriving at the end components after much shorter time of simulation (see Fig. S4 with associated discussion in the ESI†). The rather odd end product of  $\text{AuI}(\text{I}_2)$  can most likely be regarded as a product of how the scene of chemistry/composition was set in the simu-

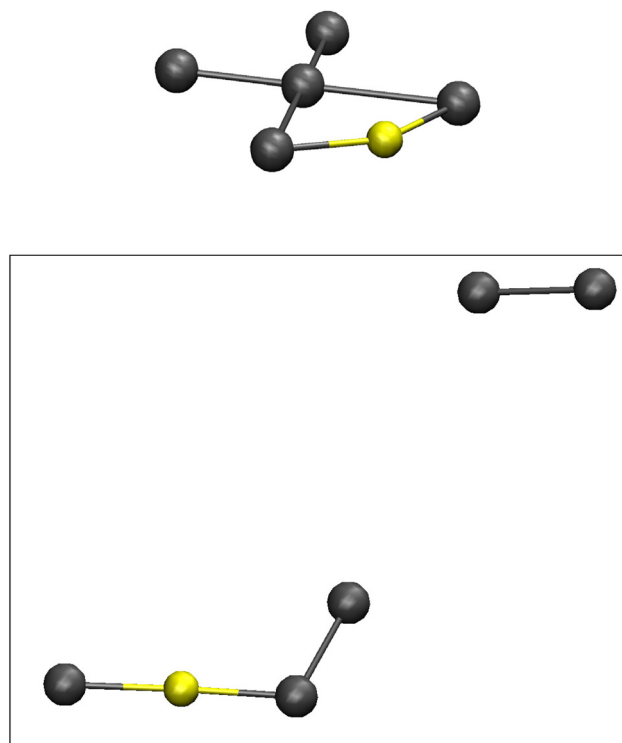


**Fig. 7** The initial  $\text{Au}\cdot\text{I}_4^-$  model as obtained from static geometry optimization (top), and a snapshot of the end products after approximately 60 ps simulation; iodine (grey), gold (yellow).

lations; inclusion of further electron donors or Lewis acids, *viz.* more iodide ions, will produce more common gold-iodide complexes together with more common polyiodide building blocks. The addition of one further iodide ion to the molecular dynamics system results in what can be described a more regular and linear gold(i) complex with the two ligands comprising one iodide ion and the  $\text{I}_4^-$  complex. At 600 °C the additional iodide ion and the thermally induced dynamics splits off one  $\text{I}_2$  unit leaving an  $\text{AuI}(\text{I}_3)$  complex behind showing occasional further extrusion of  $\text{I}_2$ . One further iodide ion in two separate entities, one linear  $\text{AuI}_2^-$  complex and the quite stable square-planar  $\text{I}_4^-$  penta-iodide complex. In this context, it can be mentioned that the only compound we have found in the literature that structurally offers a fragment close to an  $\text{I}_4^-$  unit displays a complex one-dimensional structure of the composition  $[\text{Ag}_5\text{I}_6^-]_n$  containing rather flat, pentagonal pyramidal hexaiodide units bridged by the  $\text{Ag}^+$  cations.<sup>31</sup> The I-I distances from the central iodine atom in this pentagonal pyramid spans 2.92 to 3.01 Å, but the typically encountered Ag-I distances indicate that the interesting hexaiodide configuration is coincidental, emerging as result of the Ag-I coordination in the complex cage structure.

The main conclusion is that gold and iodine forms a platform for much interesting chemistry involving a large flexibility regarding both oxidation states and coordination geometries.



## Conclusions

The current study shows that the  $\text{AuI}_4^-$ -like coordination complex of  $\text{II}_4^-$  indeed represents a local minimum on the penta-iodide PES. It is less stable than the V-shaped form typically found in solid penta-iodide compounds and should therefore be regarded as meta-stable. No straightforward pathway of transformation between the square-planar and V-shaped forms could be identified. However, the inclusion of attached cations to the square-planar  $\text{II}_4^-$  complex triggers decomposition into smaller polyiodide building blocks. This may hint to why the coordination compound version of the penta-iodide to our knowledge so far has not been identified in solid polyiodide compounds. The intrinsic stability of the square-planar  $\text{II}_4^-$  version suggests that it should be possible to isolate also this form of the penta-iodide system providing that proper synthetic conditions are applied. Two synthetic strategies appear most straightforward: either using rather large and weakly coordinating organic cations or alternatively (Fig. 7) smaller polarizing cations in combination with a strongly solvating, polar solvent.

## Conflicts of interest

There are no conflicts of interest to declare.

## Acknowledgements

The current work was funded by a grant from the Swedish Research Council (2020-06701).

## References

- P. H. Svensson and L. Kloo, *Chem. Rev.*, 2003, **103**, 1649–1684.
- L. Kloo, in *Comprehensive Inorganic Chemistry II*, ed. J. Reedijk and K. Poepelmeier, Elsevier, Oxford, 2013, ch. 1.08, vol. 1, pp. 233–249.
- J. H. Stenlid and T. Brinck, *J. Am. Chem. Soc.*, 2017, **139**, 11012–11015.
- L. Kloo, J. Rosdahl and P. H. Svensson, *Eur. J. Inorg. Chem.*, 2002, 1203–1209.
- T. A. Shestimerova, A. V. Bykov, A. N. Kuznetsov, A. Y. Grishko, Z. Wei, E. V. Dikarev and A. V. Shevelkov, *Z. Anorg. Allg. Chem.*, 2022, **e202200039**, 1–7.
- Cambridge Structural Database (CSD, <https://www.ccdc.cam.ac.uk/>).
- S. Yu and J. S. Ward, *Dalton Trans.*, 2022, **51**, 4668–4674.
- J. Linnera, S. I. Ivlev, F. Kraus and A. J. Karttunen, *Z. Anorg. Allg. Chem.*, 2019, **645**, 284–291.
- W.-L. Li, H.-T. Liu, T. Jian, G. V. Lopez, Z. A. Piazza, D.-L. Huang, T.-T. Chen, J. Su, P. Yang, X. Chen, L.-S. Wang and J. Li, *Chem. Sci.*, 2016, **7**, 475–481.
- S. Pohl, W. Saak and B. Krebs, *Z. Naturforsch.*, 1985, **40B**, 251–257.
- S. Seidel and K. Seppelt, *Science*, 2000, **290**, 117–118.
- M. J. Frisch, G. W. Trucks, H. B. Schlegel, G. E. Scuseria, M. A. Robb, J. R. Cheeseman, G. Scalmani, V. Barone, G. A. Petersson, H. Nakatsuji, X. Li, M. Caricato, A. V. Marenich, J. Bloino, B. G. Janesko, R. Gomperts, B. Mennucci, H. P. Hratchian, J. V. Ortiz, A. F. Izmaylov, J. L. Sonnenberg, D. Williams-Young, F. Ding, F. Lipparini, F. Egidi, J. Goings, B. Peng, A. Petrone, T. Henderson, D. Ranasinghe, V. G. Zakrzewski, J. Gao, N. Rega, G. Zheng, W. Liang, M. Hada, M. Ehara, K. Toyota, R. Fukuda, J. Hasegawa, M. Ishida, T. Nakajima, Y. Honda, O. Kitao, H. Nakai, T. Vreven, K. Throssell, J. J. A. Montgomery, J. E. Peralta, F. Ogliaro, M. J. Bearpark, J. J. Heyd, E. N. Brothers, K. N. Kudin, V. N. Staroverov, T. A. Keith, R. Kobayashi, J. Normand, K. Raghavachari, A. P. Rendell, J. C. Burant, S. S. Iyengar, J. Tomasi, M. Cossi, J. M. Millam, M. Klene, C. Adamo, R. Cammi, J. W. Ochterski, R. L. Martin, K. Morokuma, O. Farkas, J. B. Foresman and D. J. Fox, *Gaussian 16 Rev. C.01*, Wallingford, CT, 2016.
- D. Figgen, G. Rauhut, M. Dolg and H. Stoll, *Chem. Phys.*, 2005, **311**, 227–244.
- K. A. Peterson and C. Puzzarini, *Theor. Chem. Acc.*, 2005, **114**, 283–296.
- K. A. Peterson, B. C. Shepler, D. Figgen and H. Stoll, *J. Phys. Chem. A*, 2006, **110**, 13877–13883.
- T. Yanai, D. Tew and N. Handy, *Chem. Phys. Lett.*, 2004, **393**, 51–57.
- A development of University of Karlsruhe and Forschungszentrum Karlsruhe GmbH, 1989–2007, available from <https://www.turbomole.com>, 2017, TURBOMOLE V.7.2.
- A. D. Becke, *J. Chem. Phys.*, 1993, **98**, 5648–5652.
- F. Weigend, *Phys. Chem. Chem. Phys.*, 2006, **8**, 1057–1065.
- F. Weigend and R. Ahlrichs, *Phys. Chem. Chem. Phys.*, 2005, **7**, 3297–3305.
- I. S. Ufimtsev and T. J. Martinez, *J. Chem. Theory Comput.*, 2009, **5**, 2619–2628.
- A. V. Titov, I. S. Ufimtsev, N. Luehr and T. J. Martinez, *J. Chem. Theory Comput.*, 2013, **9**, 213–221.
- C. Bannwarth, E. Caldeweyher, S. Ehlert, A. Hansen, P. Pracht, J. Seibert, S. Spicher and S. Grimme, *Wiley Interdiscip. Rev. Comput. Mol. Sci.*, 2020, **11**, 1–49.
- C. Bannwarth, S. Ehlert and S. Grimme, *J. Chem. Theory Comput.*, 2019, **15**, 1652–1671.
- L. Martinez, R. Andrade, E. G. Birgin and J. M. Martinez, *J. Comput. Chem.*, 2009, **30**, 2157–2164.
- E. D. Glendening, J. K. Badenhoop, A. E. Reed, J. E. Carpenter, J. A. Bohmann, C. M. Morales, P. Karafiloglou, C. R. Landis and F. Weinhold, *NBO 7.0*, 2018.
- W. Humphrey, A. Dalke and K. Schulten, *J. Mol. Graph.*, 1996, **14**, 33–38.
- T. A. Keith and J. M. Millam, *GaussView 6.1*, 2016.
- C. G. Pimentel, *J. Chem. Phys.*, 1951, **19**, 446–448.
- R. J. Hach and R. E. Rundle, *J. Am. Chem. Soc.*, 1951, **73**, 4321–4324.
- X. Jin, K. Tang, W. Liu and Y. Tang, *Heteroat. Chem.*, 1995, **6**, 41–43.

